The impact of vacuum pressure on the effectiveness of SiO_2 impregnation of spruce wood

Lemaire-Paul, Mathieu; Beuthe, Callisto Ariadne; Riahinezhad, Marzieh; Reza Foruzanmehr, M.

Publisher's version / Version de l'éditeur:
https://doi.org/10.1007/s00226-022-01448-0
Wood Science and Technology, 57, 1, pp. 147-171, 2022-12-01

Wood Science and Technology (2023) 57:147–171
https://doi.org/10.1007/s00226-022-01448-0

ORIGINAL

The impact of vacuum pressure on the effectiveness of SiO_2 impregnation of spruce wood

Mathieu Lemaire-Paul[1] · Callisto Ariadne Beuthe[1] · Marzieh Riahinezhad[2] · M. Reza Foruzanmehr[1]

Received: 1 August 2022 / Accepted: 13 December 2022 / Published online: 31 December 2022

Abstract

Wood is a widely used construction material that has many advantageous properties. However, it suffers from weaknesses such as low-dimensional stability and low durability in humid environments. These issues are associated with the porous vascular structure of wood that leads to a high water uptake capacity. This research aims to reduce the water uptake capacity of spruce wood by dip-coating samples in an aqueous colloid of silicon dioxide (SiO_2) nanoparticles. SiO_2 is a dense ceramic material with good chemical stability. It is readily available and affordable, making it an excellent candidate for this application. This study investigates the effect of SiO_2 impregnation on the physico-mechanical properties of spruce wood. Density measurements, water uptake tests, microscopy examination, thermogravimetric analysis, and dynamic mechanical analysis were conducted on non-treated and SiO_2-treated spruce wood samples. Quantitative and qualitative analyses demonstrated that SiO_2 impregnation performed under higher vacuum pressure was more effective compared to the atmospheric condition and exhibited a greater presence of SiO_2 in the wood's vascular system. SiO_2 impregnation under vacuum pressure demonstrated an effective increase in the density of the wood. It also reduced the porosity, which led to a significant reduction in the water uptake of the spruce wood. The analysis of the wood viscoelastic properties revealed that SiO_2 impregnation under atmospheric and vacuum conditions triggered two different reinforcing mechanisms. The results showed that a significant improvement of the spruce wood storage and loss moduli could be achieved when impregnation was performed at the highest vacuum pressure of −90 kPa.

✉ M. Reza Foruzanmehr
mforuzan@uottawa.ca

[1] Department of Civil Engineering, University of Ottawa, 161 Louis Pasteur St., Room A022 (CBY), Ottawa, ON K1N 6N5, Canada

[2] Construction Research Center, National Research Council Canada, 1200 Montreal Road, Ottawa, ON K1A 0R6, Canada

Introduction

Wood is a naturally occurring engineering material that features a high specific strength as well as excellent thermal insulating properties (Brunner 2000; Burrows 2013). These factors, along with the environmental sustainability and short construction time of wood (Burrows 2013), have made it an attractive material in the construction industry (Burrows 2013; UPLAND 2017). Despite numerous advantages, wood also has some drawbacks. First, it has low durability in alkaline environments due to the presence of cellulose in its structure. Cellulose is a hydrophilic polymer with weak glycosidic bonds susceptible to hydrolysis (Di Blasi et al. 2009). Second, the viscoelastic behaviour of this hydrophilic polymer makes it prone to low-dimensional stability (Olsson and Salmén 1997; Irle et al. 2010). Water molecules can act as a plasticizer between the long cellulose molecular chains and introduce spaces that induce swelling. Moreover, wood possesses a porous structure with many lumens (tubular cavities inside the wood fibers). This creates a pathway for water to penetrate through capillary action (Rowell and Banks 1985). Third, the mechanical properties of wood are dependent on its moisture content. Higher moisture content leads to a lower storage modulus, higher loss modulus, and higher ductility (Greer and Pemberton 2020). Finally, wood is susceptible to attack by biological agencies such as fungi and insects (Illston and Domone 2001). The biological deterioration of wood strongly depends on the presence of moisture in its structure.

One of the best-known solution to help prevent a high water uptake level in wood and increase its durability is to modify the wood surface with superficial coatings using water repellents and physico-chemical treatments. These treatments usually involve the implementation of toxic chemical mixtures, consisting of a binder and a water repellent component such as wax (Williams and Feist 1999). However, these treatments can only create a hydrophobic surface that reduces the rate of water uptake (Rowell and Banks 1985). They do not significantly decrease the water uptake capacity of wood due to the incompatibility of hydrophobic products with the hydrophilic nature of wood. They cannot entirely obstruct the vascular system of wood and leave a gap for water to penetrate (Denes et al. 1999). Over time, treated wood will swell as much as non-treated wood (Rowell and Banks 1985). Furthermore, the performance of physico-chemical treatments is dependent on the environmental conditions the wood is subjected to, and the coating product may decay or be washed away over time (Beaulieu and Biermeier 2020). Consequently, such coatings need to be reapplied over the years to maintain optimal performance (Beaulieu and Biermeier 2020). Other prominent processes consist of chemical wood surface modification such as acetylation or furfurylation. These processes involve transforming the available hydroxyl groups of wood into hydrophobic groups (for example, acetate), which reduce wood reactivity with water. Nevertheless, these processes are time-consuming, and most are unsuitable for North-American wood species. Additionally, these processes usually have adverse effects on the mechanical properties of wood.

These shortcomings could be mitigated by homogenously coating and impregnating wood with a dense material to obstruct its vascular system (Grosse et al.

2018). Ceramic nanoparticles in an aqueous colloid state can be used to fill this porous vascular structure (Boulos et al. 2017). Silica (SiO_2) is an abundant inert ceramic with high fire resistance (Boulos et al. 2017; Bak et al. 2018). It also exhibits an acceptable resistance to alkaline environments (Shi et al. 1989; da Silva et al. 2017). These properties make SiO_2 colloids ideal candidates for an impregnation process. Through this process, the wood imbibes a colloidal solution through the vascular system. As the solvent evaporates, the nanoparticles agglomerate, fill the lumens, and obstruct the vascular structure.

Some research has already been conducted in this area. In these studies, the wood was successfully impregnated with SiO_2 colloids under vacuum, and the physical and mechanical properties of the wood were characterized (Xu et al. 2020; Zhang et al. 2019; Przystupa et al 2020; Lin and Feng 2012). However, none of these studies investigated the use of vacuum pressure to increase the effectiveness of SiO_2 impregnation. Accordingly, the novelty of this research is to study the effect of vacuum pressure on the effectiveness of the impregnation process for finding the optimal impregnation condition under vacuum. Moreover, research has yet to reveal the impact of vacuum-aided impregnation on the viscoelastic properties of wood.

The focus of this research is to overcome wood's weakness by reducing its water uptake capacity through an impregnation process. The primary objective is to investigate the effect of vacuum on the SiO_2 impregnation of wood by measuring the density and water uptake capacity of samples before and after impregnation treatment under atmospheric and three vacuum pressures to find the optimal vacuum impregnation pressure. The secondary objective of this work is to identify changes in the viscoelastic properties of wood as a result of SiO_2 vacuum-aided impregnation. This study could encourage new innovations for multiple materials and applications where the simultaneous elastic behaviour of wood and its damping energy is needed. It could also pave the way for research on the synergistic effects of SiO_2 impregnation on the water uptake and viscoelastic behaviour of wood.

Methodology

Materials

The samples used in this study were prepared from spruce wood of the *Picea glauca* species, commonly known as Canadian spruce or White spruce. Spruce is the most frequently used type of wood in eastern Canada. LUDOX HS-40 colloidal silica, a water-based colloidal suspension of nano-silica, was used as an impregnation solution. This suspension contained a 40% solution of 12 nm SiO_2 particles, with a pH of 9.5, and has an aqueous density of 1.3 g/cm^3 at 25 °C. The solution was purchased from Sigma-Aldrich.

Table 1 Samples designations and descriptions

Sample designation	Description
NT	Non-treated
ATM	SiO_2 impregnated wood at atmospheric pressure
− 30 kPa	SiO_2 impregnated wood under a vacuum pressure of − 30 kPa
− 60 kPa	SiO_2 impregnated wood under a vacuum pressure of − 60 kPa
− 90 kPa	SiO_2 impregnated wood under a vacuum pressure of − 90 kPa

Sample preparation

The wood specimens were cut and sanded to the required dimensions for the tests and characterization techniques. The wood specimens contained both earlywood and latewood. The sample's dimensions (length × width × thickness) were: (25 mm × 10 mm × 2 mm) for dynamic mechanical analysis, (33 mm × 14.5 mm × 14.5 mm) for pycnometry, and (3 mm × 2 mm × 1 mm) for tensiometry. The samples were progressively sanded using sandpaper with grits of 80, 100, 120, 220, and 600 to remove any residues on the specimens and reach a consistent surface roughness. The length of the samples was cut along the longitudinal wood fiber axis, and the base cross-section (width and thickness) was in the tangential-radial plane. The samples were placed in an oven at 103 °C for 24 h prior to the tests to dry them in order to minimize their humidity content.

Impregnation process

The wood specimens were impregnated with the SiO_2 colloid using a dip-coating technique. Although the samples can naturally absorb the solution, air entrapped within the macropores will impede the effective impregnation of the sample. To mitigate this issue and improve the effectiveness of the impregnation, the process was conducted under vacuum pressure using the Buehler Cast-N-Vac 1000 vacuum chamber. The samples were impregnated under different negative pressures of − 30, − 60, and − 90 kPa and also under atmospheric conditions for one hour. Following the impregnation process, the samples were placed in an oven at 50 °C for one hour and 100 °C for five minutes to accelerate the agglomeration of the SiO_2 nanoparticles inside the vascular system.

Sample designations and descriptions

Table 1 presents the sample designations and their respective descriptions. These designations will be used throughout the tables and figures presented in this paper.

Characterizations

Scanning electron microscopy

The impregnated samples were analyzed using a scanning electron microscope (SEM) to examine the effect of vacuum on the diffusion of SiO_2 particles into the vascular system of wood. The samples were cold mounted and halved.[1] Prior to SEM analysis, all samples were polished and coated by a vapour-deposited 20 µm layer of Pd–Au. The microscopy was carried out using a JSM-7500F FESEM at 2–3 kV. Secondary electron detectors and energy dispersive spectroscopy (EDS) were used for this characterization method.

Transmission electron microscopy

Treated and non-treated samples were analyzed with a transmission electron microscope (TEM) to assess the effect of vacuum pressure on the presence of SiO_2 nanoparticles in the lumens of the samples. The cross-sections were prepared following the method used for biological specimens (Luft 1961). The samples were sectioned at 80 nm by a microtome with a diamond blade. The sections were stained with a solution of uranyl acetate and were observed on a copper grid at 80 kV with TEM. All microscopy was carried out using a Hitachi H-7500 machine at 80 kV.

Density measurements

The density of samples before and after impregnation was determined using a micromeritics gas pycnometer (AccuPyc II 1340). Helium was used for the measurements. The density of each sample was measured three times to determine the mean value both before and after impregnation. Five samples were tested for each impregnation condition.

Water uptake measurements

The water uptake of samples before and after SiO_2 impregnation was determined using the Washburn method for porous materials with a force balance tensiometer (DCA-100F First Ten Angstroms). In order to reach the wood saturation point quickly, small specimens of $3 \times 2 \times 1$ mm with a mass between 2 and 3 mg were tested. The saturation point was determined by identifying the plateau section of the water absorption graph. Five samples of each impregnation condition were tested. Each specimen was inserted into a spring-loaded immersion clip and brought into contact with distilled water. Starting from the time of immersion, the mass uptake was recorded every second for a total of 600 s, and the water uptake (Weight %) was calculated as follows with Eq. (1).

[1] A tangential-radial cross-sectional slice from the longitudinal center of the sample was taken.

$$\text{Weight\%} = \frac{100 \times \left(M_{\text{wet}} - M_{\text{dry}}\right)}{M_{\text{dry}}} \tag{1}$$

where M_{wet} is the mass of the samples with the absorbed water and M_{dry} is the mass of the samples in a dry state.

To quantify the water uptake reduction at saturation after impregnation, the reduction magnitude (R_m) was calculated as follows with Eq. (2).

$$R_m = \text{Weight\% before impregnation} - \text{Weight\% after impregnation} \tag{2}$$

The Weight% before and after impregnation were both taken at saturation such as at $\sqrt{t}/L = 7$, where t is the time (s), and L is the length of the sample (mm). The $\sqrt{t}/L$ represents the x-axis, and the weight % represents the y-axis of the water uptake graph (see "Appendix A" in Electronic Supplementary Information). All samples showed a plateau and thus saturation at $\sqrt{t}/L = 7$ in the water uptake graph, hence why it was selected as the reference point for analysis and comparison.

Wood is a natural product with an irregular structure and can exhibit a high degree of variability in its properties. To offset the effects of this variability on the test results, the following experimental process was employed. First, each sample in its non-treated dry state was tested to saturation. Then the sample was dried in an oven at 103 °C for 24 h. Next, the same sample, now dry, was impregnated with SiO_2 and tested to saturation again. The procedure was repeated respectively for all the SiO_2 impregnation conditions. This procedure ensures that the differences in water uptake are induced by the impregnation conditions rather than the inherent irregularity in the sample structure. As a result, with the above procedure, it was possible to compare the water uptake capacity of the same samples before and after impregnation and calculate the reduction magnitude using Eq. (2).

Simultaneous thermal analysis

Thermogravimetric analysis (TGA) coupled differential scanning calorimetry (DSC) was carried out using a TA Instrument Q600 V8.3 under a nitrogen atmosphere with a heating rate of 10 °C/min. The weight loss traces were recorded as a function of temperature in the range of 20–500 °C.

Dynamic mechanical analysis

Treated and non-treated wood samples were tested in a dry state using dynamic mechanical analysis (DMA). Five samples of each impregnation condition were tested. The test apparatus was equipped with a 3-point bending clamp setup. The effect of the vacuum pressure impregnation process on the viscoelastic properties of wood (i.e., storage modulus, loss modulus, and tan δ) was studied. The viscoelastic properties were measured before and after each impregnation. Multi-strain tests were carried out using a TA Instruments DMA Q800 testing machine set to a frequency of 1 Hz

and a temperature range of 5–40 °C. The temperature range was selected to analyze the effect of impregnation at ambient, below ambient, and above ambient temperature.

Statistical analysis

A two-sample *t*-test was applied to compare the mean values of each key property (Livingston 2004). A confidence interval of 95% was considered as long as the P-value was below 0.05, indicating significant differences among the values.

Results and discussion

Scanning electron microscopy

Figure 1 presents micrographs of the scanning electron microscopy (SEM) and energy dispersive spectroscopy (EDS) analyses performed on the cross-section of halved samples. Because the middle of a sample is at the maximum distance from the sample extremities, the presence of SiO_2 particles in the micrographs represents the maximum depth of diffusion in the vascular system of the wood. The EDS analyses were performed to survey the dispersion of silica particles in the wood structure. Figure 1a and b shows that under atmospheric pressure, only a few lumens are filled with SiO_2. Most lumens remain empty due to an abundance of entrapped air present in the open pores, preventing the SiO_2 colloid from permeating into the pores. EDS analysis revealed that under atmospheric pressure, the SiO_2 remains primarily on the surface of the specimen. In this case, the colloidal solution permeates into the wood cavities through capillary action. However, the capillary pressure was not high enough to displace the entrapped air and allow the SiO_2 colloid to permeate into the core of the wood structure, resulting in a low depth of SiO_2 particle diffusion. In addition, the colloid (weakly alkaline solution with pH 9.2–9.9) precipitated on the surface, allowing the particles to aggregate and form a solid film on the surface of the wood. This phenomenon occurs because wood is generally acidic in nature (Illston and Domone 2001) and neutralizes the alkaline colloid (Jiang et al. 2018), causing the SiO_2 particles to precipitate. The SEM micrograph of the ATM sample also reveals the lack of diffusion of SiO_2 particles in the longitudinal direction and a shallow diffusion of particles at the surface in the radial direction. Figure 1c and d shows that when a vacuum pressure of − 30 kPa was used, there was a slight increase in the depth of diffusion of the particles into the wood vascular structure. Figure 1e and f shows that changing the vacuum pressure to − 60 kPa improved the impregnation process. A vacuum pressure of − 60 kPa helped the SiO_2 colloid permeate further into the wood vascular structure, but it was not effective enough to eliminate the entrapped air and fill the open pores. Figure 1g and h show that under a vacuum pressure of − 90 kPa, the majority of the lumens are clogged with SiO_2 particles. These micrographs qualitatively confirmed that using a vacuum pressure of − 90 kPa helped remove the entrapped air. This effectively enhanced the impregnation process and reduced the porosity by obstructing the vascular system of the wood with the agglomerated SiO_2 particles.

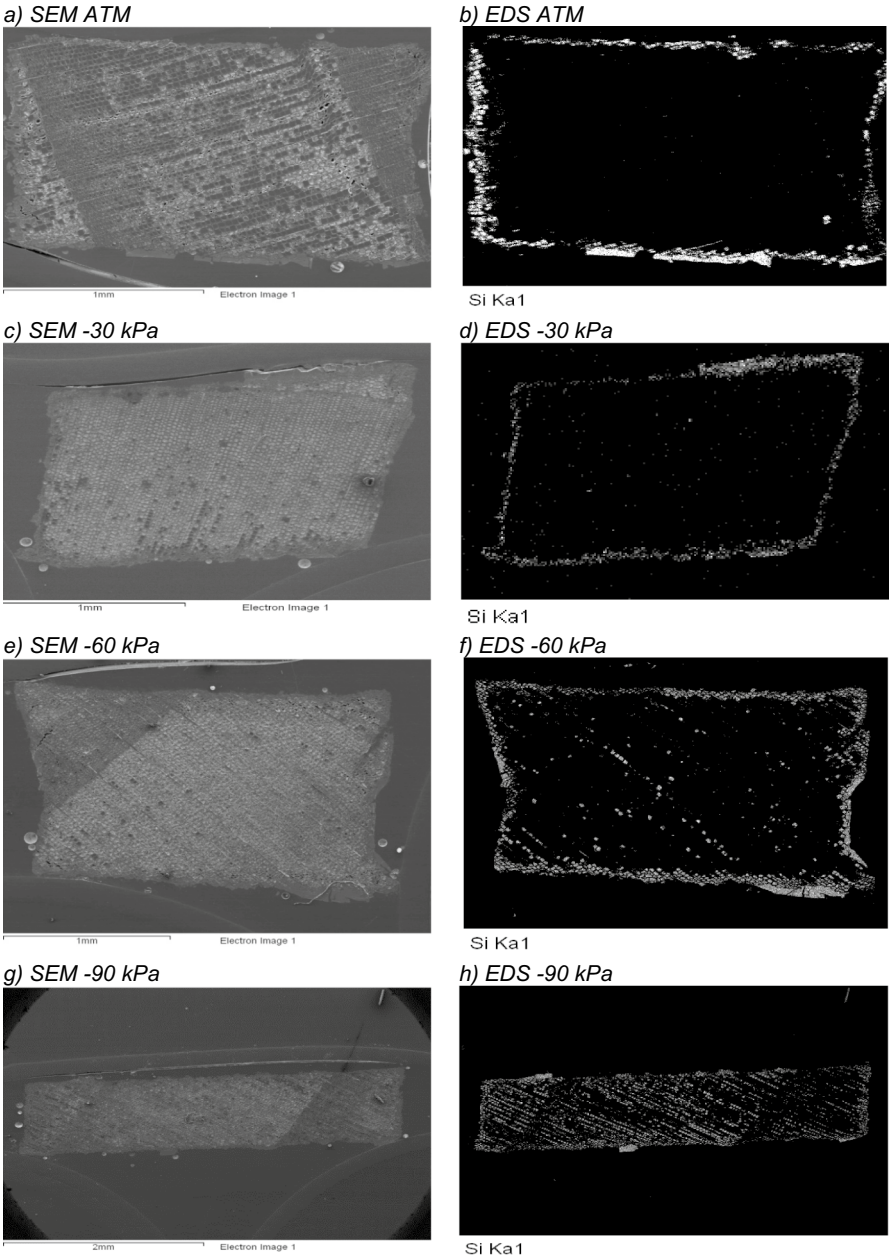

Fig. 1 SEM, EDS micrographs of **a**, **b** ATM. **c**, **d** – 30 kPa. **e**, **f** – 60 kPa. **g**, **h** – 90 kPa

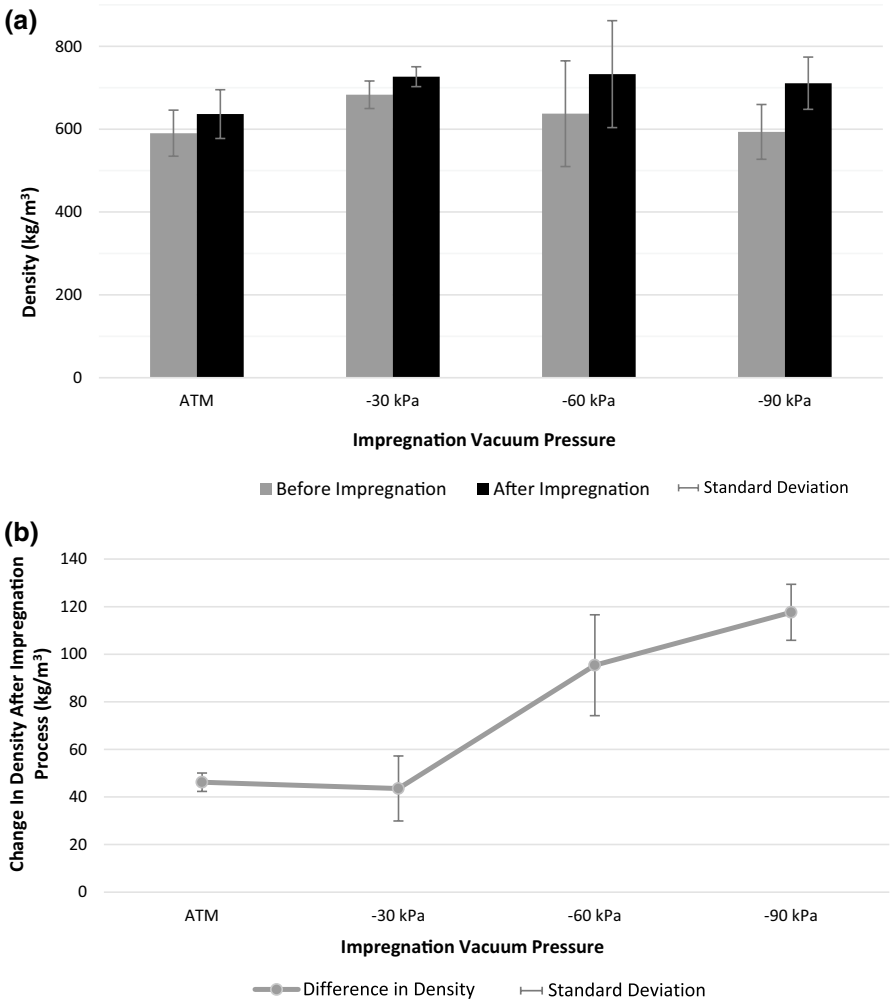

Fig. 2 **a** Density of the samples before and after the impregnations. **b** Difference in density before and after the impregnations

Density measurements

Figure 2a and b shows the results of the density tests conducted on the SiO_2 impregnated samples under atmospheric pressure and three vacuum pressures compared to their non-treated state. As shown in Fig. 2a, the impregnation process has increased the density in all samples, regardless of the impregnation vacuum pressure. Moreover, the samples impregnated using a vacuum pressure of − 60 and − 90 kPa exhibited higher densities compared to the samples impregnated at atmospheric pressure. Furthermore, samples impregnated at a vacuum pressure of − 90 kPa experienced the highest density increase among all of the SiO_2 impregnated samples. Figure 2b

shows the change in the density of a given sample before and after SiO_2 treatment. Impregnation under vacuum increased the effectiveness of the SiO_2 impregnation by a factor of 2.6. The trend shown in Fig. 2b indicates that a greater change in density can be expected with increasing vacuum pressure.

Table 2 presents the statistical analysis conducted to compare the density of the treated and non-treated samples. The *P* values of the statistical analysis revealed that the change in density before and after the impregnation was significant for all samples. Moreover, the difference in density between all of the treated samples was statistically significant except for the difference between the ATM and − 30 kPa samples. Subjecting wood to a vacuum during impregnation helps remove the entrapped air in the vascular system and pores and facilitates the impregnation process. The vacuum pressure of − 30 kPa did not appear to be strong enough to effectively remove the entrapped air. Therefore, the SiO_2 colloid could not penetrate into the core of the wood vascular structure. The effect of vacuum pressure on the depth of penetration of the SiO_2 particles in the wood structure is explored more in depth in Sect. "Scanning electron microscopy".

Water uptake measurements

Figure 3a and b shows water uptake test results before and after SiO_2 impregnation under atmospheric pressure and three vacuum pressures. The results show that the samples impregnated under − 90 kPa exhibited the highest water weight % reduction (732 wt% [7.32 ×]), and hence achieved the lowest water uptake at saturation after impregnation. This water uptake reduction is significantly higher than that of the ATM samples (452 wt% [4.52 ×]), the -30 kPa samples (475 wt% [4.75 ×]), and the − 60 kPa samples (478 wt% [4.78 ×]). This significant decrease in water uptake at saturation is caused by the reduction of void volume in the wood structure. The SiO_2 impregnation successfully obstructed the vascular system of the wood and effectively reduced its capacity to absorb water. The SiO_2 impregnated samples under a vacuum pressure of − 90 kPa exhibited 7.32 and 2.80 times less water uptake than non-treated samples and impregnated samples under atmospheric pressure conditions, respectively. Impregnation under atmospheric conditions is impeded by the presence of entrapped air within the lumens which prevents the SiO_2 from permeating and fully obstructing the lumens. This suggests that ATM impregnation only coats the surface of the wood and is not as effective as impregnation under vacuum conditions (see also SEM analysis in Sect. "Scanning electron microscopy"). These results also confirmed the results of the density tests, where a vacuum pressure of − 90 kPa provided the most effective impregnation condition to achieve the highest density increase among all of the SiO_2 impregnated samples.

Table 3 presents the statistical analysis conducted to compare the water uptake capacity of treated and non-treated samples. Non-treated samples showed a larger standard deviation for water uptake at saturation than treated samples. When the samples were put in contact with water, the ability of water to enter the wood pores was dependent on the size of the pores and the amount of air entrapped within them. The observed variation in water uptake is caused by the naturally occurring range

Table 2 Statistical analysis of density tests

Before			After			|Before – after|	
Type	Average density kg/m^3	Standard deviation	Type	Average density kg/m^3	Standard deviation	Average density kg/m^3	Standard deviation
Before ATM	590	6	After ATM	636	2	46	4
Before – 30 kPa	683	18	After -30 kPa	727	8	44	14
Before – 60 kPa	637	73	After -60 kPa	733	74	96	21
Before – 90 kPa	593	37	After -90 kPa	711	34	118	12

Sample comparison	Z score and *P* value	Statistical significance
Before ATM versus after ATM	Z score = – 9.843 *P* value = < 0.05	Significant
Before – 30 kPa versus after – 30 kPa	Z score = – 3.773 *P* value = < 0.05	Significant
Before – 60 kPa versus after – 60 kPa	Z score = – 2.603 *P* value = < 0.05	Significant
Before – 90 kPa versus after – 90 kPa	Z score = – 5.710 *P* value = < 0.05	Significant
ATM versus – 30 kPa	Z score = 0.314 *P* value = 0.753	Insignificant
– 30 kPa versus – 60 kPa	Z score = – 4.761 *P* value = < 0.05	Significant
– 60 kPa versus – 90 kPa	Z score = – 2.497 *P* value = < 0.05	Significant

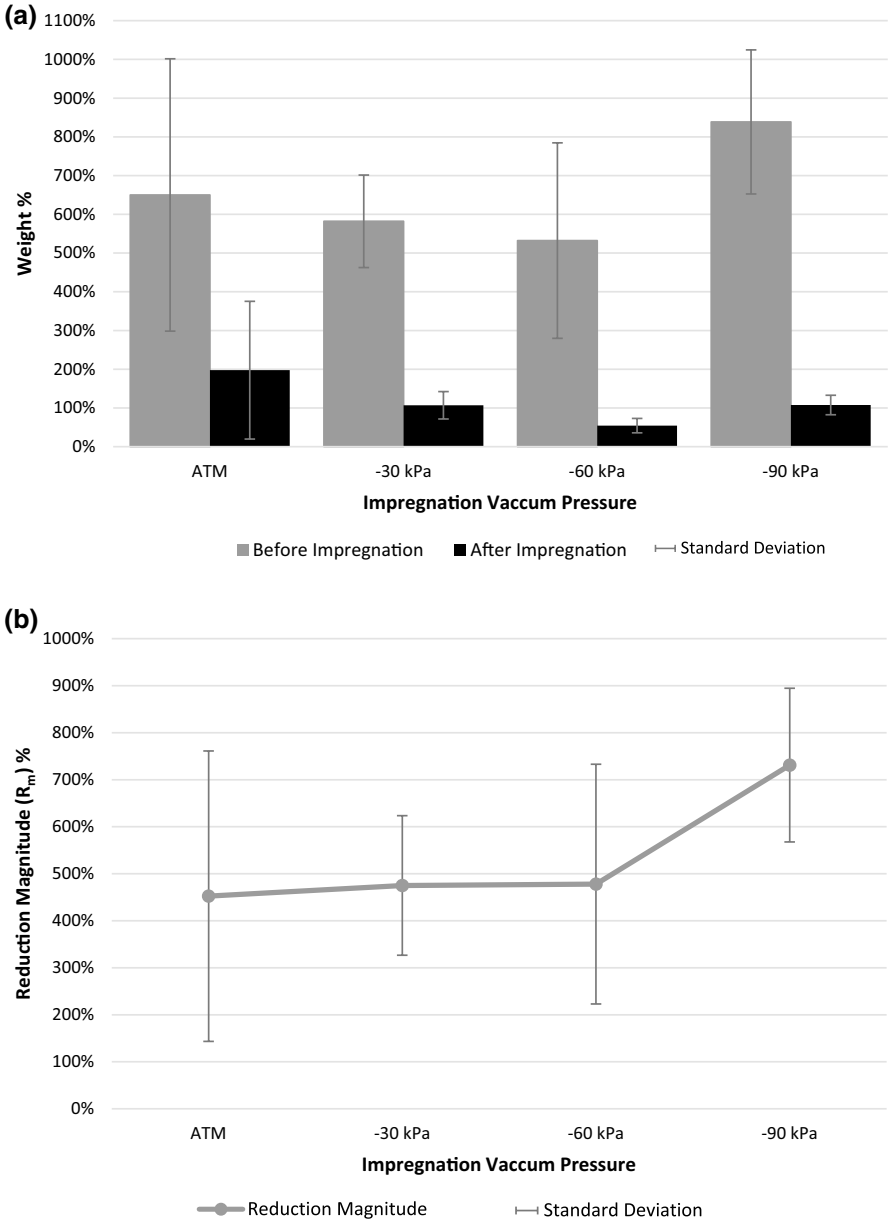

Fig. 3 **a** Water uptake capacity at $\sqrt{t}/L=7$ before and after the impregnations. **b** Reduction magnitude in water uptake capacity at $\sqrt{t}/L=7$ before and after the impregnations

of microscopic pore diameters in the non-treated samples (Prošek et al. 2015). The standard deviation of the samples after impregnation showed a significant decrease compared to the standard deviation of the same samples before impregnation. This

Table 3 Statistical analysis of water uptake tests

Before				After				|Before – after|	
Type	$\sqrt{t}/L$	Average weight%	Standard deviation	Type	$\sqrt{t}/L$	Average weight%	Standard deviation	R_m %	Standard deviation
Before ATM	7	650	352	After ATM	7	198	178	452	309
Before – 30 kPa	7	582	119	After -30 kPa	7	107	35	475	148
Before – 60 kPa	7	532	252	After -60 kPa	7	54	19	478	255
Before – 90 kPa	7	839	186	After -90 kPa	7	107	25	732	163

Sample comparison	Z score and *P* value	Statistical significance
Before ATM versus after ATM	Z score = 3.247 *P* value = < 0.05	Significant
Before – 30 kPa versus after – 30 kPa	Z score = 8.929 *P* value = < 0.05	Significant
Before – 60 kPa versus after – 60 kPa	Z score = 5.391 *P* value = < 0.05	Significant
Before – 90 kPa versus after – 90 kPa	Z score = 8.709 *P* value = < 0.05	Significant
ATM versus – 30 kPa	Z score = – 0.172 *P* value = 0.863	Insignificant
– 30 kPa versus – 60 kPa	Z score = – 0.03 *P* value = 0.980	Insignificant
– 60 kPa versus – 90 kPa	Z score = – 2.181 *P* value = < 0.05	Significant

decrease is caused by a substantial reduction in the number of microscopic pores open to the surface. The SiO_2 impregnation under negative pressure eliminated the microscopic pores through a two-stage mechanism. The vacuum evacuates the entrapped air and allows the SiO_2 colloid to permeate into the pores, inundate, and eventually clog them entirely. The standard deviation is found to be the lowest for the − 90 kPa samples. The P-values of the statistical analysis demonstrated that the difference in reduction magnitude from ATM to − 60 kPa is not significant, while the difference in reduction magnitude from − 60 to − 90 kPa is significant. The results clearly show that non-treated samples absorbed significantly more water than the treated ones under all conditions. The statistical analysis (Table 3) revealed that the SiO_2 impregnation under vacuum pressure up to − 60 kPa significantly decreased the water uptake at saturation of spruce wood compared to non-treated samples. However, there was not a statistically significant difference between these impregnated samples (i.e., impregnated samples from ATM to − 60 kPa). Enhancing the vacuum pressure from − 60 to − 90 kPa showed a statistically significant change in the water uptake at saturation. The results indicated that impregnation under a vacuum pressure of − 90 kPa was the most effective condition to reduce the water uptake at saturation of spruce wood. This level of vacuum pressure seems to represent the optimal condition needed to evacuate air and initiate the transport of SiO_2 nanoparticles into the vascular structure of spruce wood.

Transmission electron microscopy

Figure 4 shows TEM micrographs (longitudinal sections) of non-treated and − 90 kPa treated samples. The − 90 kPa vacuum was selected to represent the most effective impregnation condition versus the reference (non-treated) sample. Non-treated and − 90 kPa samples were analyzed under microscopy to reveal the presence of nanoparticles in the vascular system of the wood. The presence of SiO_2 can be observed as well as the vascular system of the spruce wood. Figure 4a and c do not show the presence of SiO_2 nanoparticles in the lumens, but the presence of dense particles is noticeable in Fig. 4b and d. These images support the results obtained in the SEM analysis and previous measurements (density and water uptake capacity). The originally empty lumens are now obstructed with SiO_2 nanoparticles, which helps reduce the water uptake.

Simultaneous thermal analysis

Figure 5 depicts the derivative thermo-gravimetry (DTG) and differential scanning calorimetry (DSC) thermograms of the SiO_2 impregnated samples within the temperature region where cellulose degrades thermally (330–350 °C), as shown by the endothermic peak in Fig. 5a. The ATM sample had the highest peak temperature and enthalpy for the degradation of cellulose of all impregnated samples. Additionally, the endothermic peak decreases as the vacuum pressure intensifies (see Table 4). As discussed in "Scanning electron microscopy" section, at atmospheric conditions, the colloid was unable to permeate deeply into the wood pores and cavities due to the

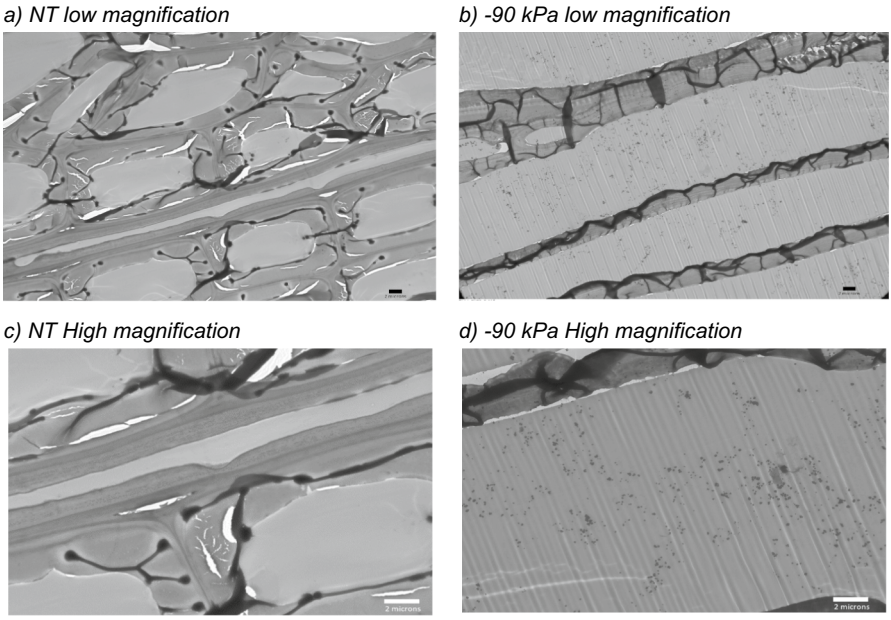

Fig. 4 TEM micrographs of NT and − 90 kPa treated wood samples

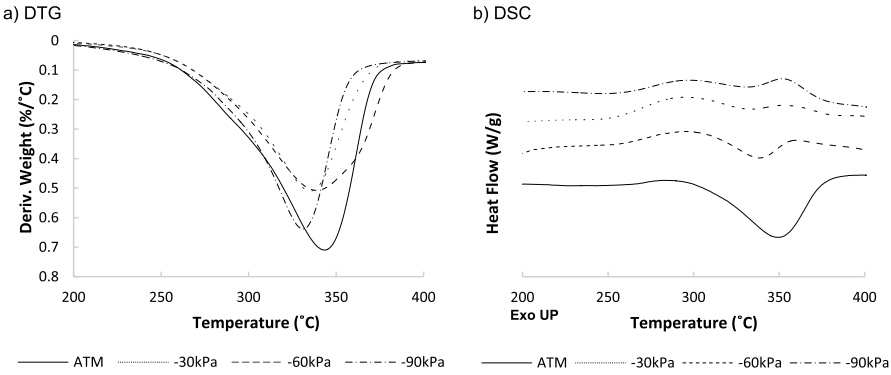

Fig. 5 DTG and DSC thermograms of SiO_2 impregnated samples

Table 4 Thermal degradation properties of the SiO_2 impregnated samples

Device	Measured parameter	ATM	− 30 kPa	− 60 kPa	− 90 kPa
TGA	Maximum mass loss temperature (°C)	344	339	335	333
DSC	Cellulose degradation temperature (°C)	349	338	332	330
	Cellulose degradation enthalpy (J/g)	48.8	11	3.4	3.1

presence of entrapped air in the wood. Therefore, the cellulose was not exposed to the alkaline solution and was able to remain intact. By contrast, under vacuum pressure, the entrapped air was evacuated and allowed the alkaline colloid to diffuse into the vascular system of the wood. Consequently, the vacuum facilitated the infiltration of the liquid phase of the colloid (containing OH^- ions) through the vascular structure of the wood. This colloid can attack the glycosidic cellulose bonds and cause degradation-solubilization and the loss of properties (Borůvka et al. 2016). As a result of this chemically induced degradation, the enthalpy of the thermal degradation of cellulose decreased by 77% for the impregnated sample at − 30 kPa vacuum pressure. The sample showed a drop of 11 °C in the peak temperature of cellulose thermal degradation compared to the ATM sample. This side effect was exacerbated as the vacuum increased. However, the magnitude of the degradation of cellulose due to chemical attack reached a plateau for vacuum pressures beyond − 60 kPa. The temperature at which the samples exhibit a maximum mass loss is also used as a criterion to examine the degradation of lignocellulosic materials (Foruzanmehr et al. 2017). These temperatures confirm that the negative effect of the vacuum impregnation of wood with the SiO_2 colloid was less pronounced at a vacuum pressure of − 90 kPa.

Dynamic mechanical analysis

Figure 6 shows the storage modulus, loss modulus, and tan δ before and after the impregnation of the wood samples. Three temperatures (ambient, below ambient, and above ambient) were selected to compare the viscoelastic properties of the samples. Tables 5 and 6 present the quantitative data along with the statistical analysis of the DMA results before and after the impregnation process respective to these three temperatures. The results showed that the SiO_2 impregnation under the atmospheric and − 90 kPa vacuum conditions caused significant alterations in the storage and loss moduli of spruce wood. Although the − 30 kPa and − 60 kPa samples exhibited noticeable changes in their viscoelastic properties, for the majority of the temperature ranges, these changes were not statistically significant compared to the samples before impregnation.

Tables 5 and 6 indicate a significant increase in the storage and loss moduli of the ATM samples at temperatures between 5 °C and 35 °C. The general performance of solid viscoelastic material indicates that an increase in storage modulus is accompanied by a decrease in loss modulus (Ferry 1980). In other words, in solid viscoelastic materials, the elastic and viscous properties measured from the storage and loss moduli, respectively, are negatively correlated. However, SiO_2 impregnation of samples at atmospheric conditions simultaneously enhanced both the elastic and viscous properties of the treated samples, likely due to the precipitation-aggregation of SiO_2 particles, as discussed in Sect. "Scanning electron microscopy". The resulting formation of a rigid layer on the surface of the samples may have reinforced the wood and caused the storage modulus to increase. Additionally, the increase in loss modulus indicates that the ability of the ATM samples to dissipate energy increased. The ATM samples formed a solid film that could dissipate energy at the interface

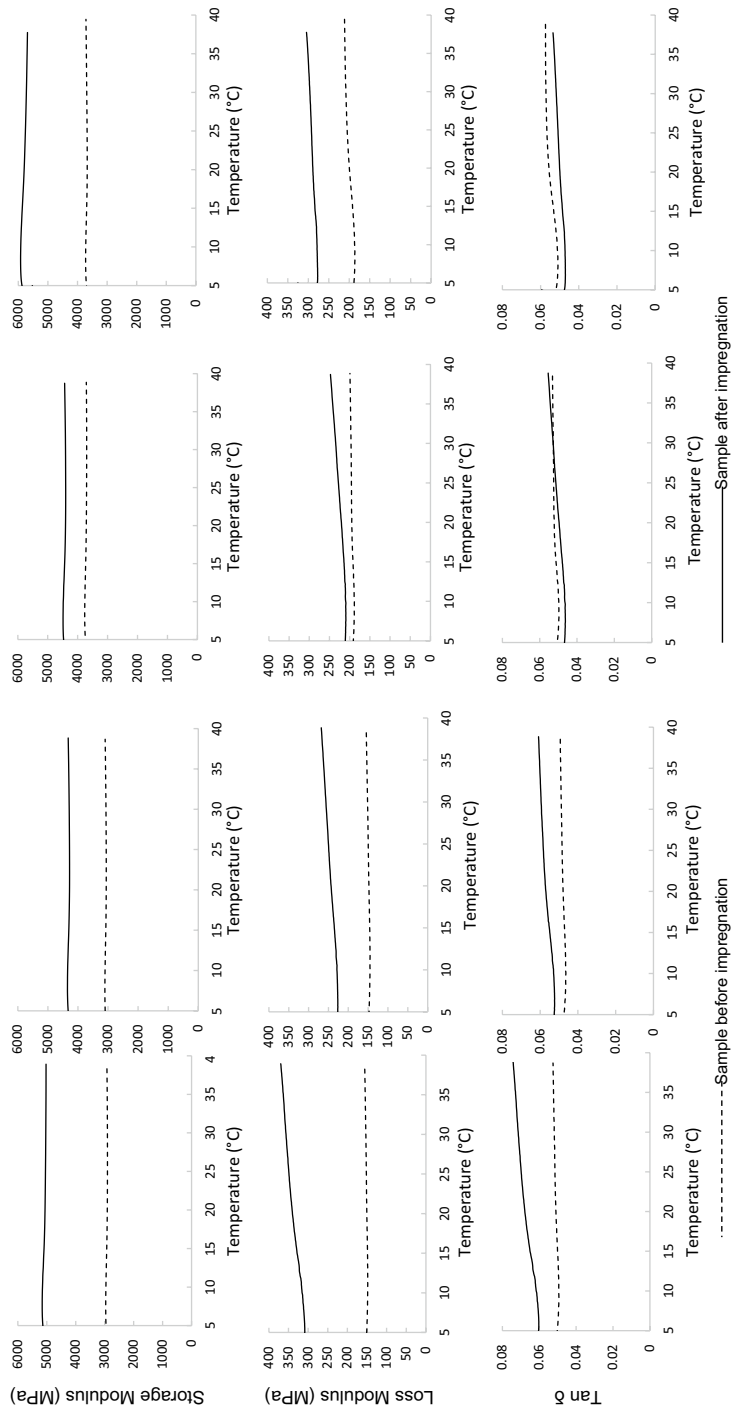

Fig. 6 DMA test results of the storage modulus, loss modulus, and tan δ before and after the impregnations

Table 5 DMA test results of the storage modulus before and after the impregnations

Impregnation condition	Average storage modulus (MPa) at 5 °C			Average storage modulus (MPa) at 25 °C			Average storage modulus (mpa) at 35 °C		
	Before	After	%Difference	Before	After	%Difference	Before	After	%Difference
ATM	2954	5136	74	2903	5044	74	2912	5026	73
−30 kPa	3094	4327	40	3060	4281	40	3083	4308	40
−60 kPa	3741	4469	19	3702	4400	19	3702	4421	19
−90 kPa	3692	5876	59	3676	5760	57	3702	5702	54
Sample comparison	Z score and *P* value		Statistical significance	Z score and *P* value		Statistical significance	Z score and *P* value		Statistical significance
ATM before versus ATM after	Z score = −3.496 *P* value = <0.05		Significant	Z score = −3.541 *P* value = <0.05		Significant	Z score = −3.502 *P* value = <0.05		Significant
−30 kPa before versus −30 kPa After	Z score = −1.644 *P* value = 0.100		Insignificant	Z score = −1.631 *P* value = 0.103		Insignificant	Z score = −1.658 *P* value = 0.097		Insignificant
−60 kPa before versus −60 kPa after	Z score = −1.221 *P* value = 0.222		Insignificant	Z score = −1.201 *P* value = 0.23		Insignificant	Z score = −1.237 *P* value = 0.216		Insignificant
−90 kPa before versus −90 kPa after	Z score = −4.093 *P* value = <0.05		Significant	Z score = −4.013 *P* value = <0.05		Significant	Z score = −3.832 *P* value = <0.05		Significant

*%Difference = ((After − Before) / Before) × 100

Table 6 DMA test results of the loss modulus before and after the impregnations

Impregnation condition	Average loss modulus (MPa) at 5 °C			Average loss modulus (MPa) at 25 °C			Average loss modulus (MPa) at 35 °C		
	Before	After	%Difference	Before	After	%Difference	Before	After	%Difference
ATM	151	308	104	152	349	130	155	363	135
−30 kPa	148	227	53	150	250	67	153	263	72
−60 kPa	191	211	10	196	228	16	198	242	22
−90 kPa	189	278	47	205	292	42	210	301	43
Sample comparison	Z score and *P* value		Statistical significance	Z score and *P* value		Statistical significance	Z score and *P* value		Statistical significance
ATM before versus ATM after	Z score = −4.370 *P* value = <0.05		Significant	Z score = −5.432 *P* value = <0.05		Significant	Z score = −5.492 *P* value = <0.05		Significant
−30 kPa before versus −30 kPa after	Z score = −1.945 *P* value = 0.0518		Insignificant	Z score = −2.240 *P* value = <0.05		Significant	Z score = −2.289 *P* value = <0.05		Significant
−60 kPa before versus −60 kPa after	Z score = −0.546 *P* value = 0.585		Insignificant	Z score = −0.877 *P* value = 0.380		Insignificant	Z score = −1.179 *P* value = 0.238		Insignificant
−90 kPa before versus −90 kPa after	Z score = −3.735 *P* value = <0.05		Significant	Z score = −3.228 *P* value = <0.05		Significant	Z score = −3.145 *P* value = <0.05		Significant

*%Difference = ((After − Before) / Before) × 100

between the film and the wood fibers through friction, as described by the stick–slip oscillation model (Martins et al. 1990).

Detailed investigations revealed that impregnation under vacuum could enhance the storage modulus of wood, but only at high vacuum pressures, since there are two competing mechanisms at work. The impregnation under vacuum is a double-edged sword. On one hand, the vacuum helps the SiO_2 particles (the solid phase of the colloid) diffuse and disperse into the vascular system of the wood. On the other hand, this process exposes the inner structure of the wood to an alkaline solution. This can cause the structure to degrade and result in a deterioration of the properties. However, this loss of rigidity (i.e., degradation) can be partially or completely compensated by the addition of SiO_2 nanoparticles depending on the strength of the vacuum to uniformly disperse the particles into the wood structure.

For example, a vacuum pressure of − 30 kPa was able to partially remove the entrapped air but was not strong enough to allow the particles to diffuse deeply into the wood vascular structure. As a result, the SiO_2 particles primarily aggregated on the surface and, similar to the ATM samples, formed a solid layer on the surface as shown in Fig. 1d. However, the infiltration of hydroxyl ions into the wood structure may have undermined the solid film reinforcing effect and made the increase in the storage modulus become insignificant. Furthermore, the results showed that the loss modulus of − 30 kPa samples increased similar to the ATM samples. This correlation could also be related to the formation of a SiO_2 film on the surface of the − 30 kPa samples. However, the change in loss modulus before and after impregnation was statistically insignificant at 5 °C, as shown in Table 6. One hypothesis to explain this phenomenon is the positive effect of the mild vacuum (− 30 kPa) on the diffusion of SiO_2 particles into the surface cavities of the wood. This penetration of the SiO_2 film into the surface openings created an integrated texture at the surface that could reduce the interfacial friction at low temperatures. The results also revealed that in the − 60 kPa samples, the effect of degradation was dominant compared to the reinforcing effect of SiO_2 impregnation, as they exhibited the minimum increase in storage modulus among all the impregnated samples.

Finally, the results showed that at − 90 kPa, the vacuum pressure was high enough to successfully remove the entrapped air in the wood structure, allowing the colloid to infiltrate through capillary action and transport the SiO_2 nanoparticles to the core of the samples. Consequently, the SiO_2 particles were uniformly dispersed in the vascular system of the spruce wood samples, leading to a significant increase in storage modulus as the voids filled with rigid SiO_2 nanoparticles. This increase in rigidity reflects the rule of mixtures in composites (Callister and Rethwisch 2018). In this case, the dominant modifying mechanism was the reinforcing effect of the impregnation and not the degradation side effect. However, the mechanism by which the loss modulus improved was different from the one shown in the ATM samples. In samples treated under − 90 kPa vacuum, the uniform dispersion of SiO_2 particles in the lumens caused the dissipation of energy through particle–particle and particle-lumen wall frictions when the samples underwent deformations. Another key observation in the viscoelastic behaviour of the − 90 kPa samples shown in Table 7 is the decrease in tan δ. Although the decrease was only significant at a temperature of 5 °C, this is the only impregnation condition that caused a statistically significant

Table 7 DMA test results of the tan δ before and after the impregnations

Impregnation condition	Average tan delta at 5 °C			Average tan delta at 25 °C			Average tan delta at 35 °C		
	Before	After	%Difference	Before	After	%Difference	Before	After	%Difference
ATM	0.0502	0.0603	20	0.0515	0.0699	36	0.0523	0.0729	40
−30 kPa	0.0473	0.0526	11	0.0484	0.0583	21	0.0491	0.0602	23
−60 kPa	0.0507	0.0467	−8	0.0525	0.0513	−2	0.0530	0.0544	3
−90 kPa	0.0519	0.0475	−9	0.0567	0.0509	−10	0.0574	0.0528	−8
Sample comparison	Z score and *P* value		Statistical significance	Z score and *P* value		Statistical significance	Z score and *P* value		Statistical Significance
ATM before versus ATM after	Z score = −4.223 *P* value = <0.05		Significant	Z score = −6.457 *P* value = <0.05		Significant	Z score = −7.019 *P* value = <0.05		Significant
−30 kPa before versus −30 kPa after	Z score = −2.201 *P* value = <0.05		Significant	Z score = −4.760 *P* value = <0.05		Significant	Z score = −4.703 *P* value = <0.05		Significant
−60 kPa before versus −60 kPa after	Z score = 1.669 *P* value = 0.0951		Insignificant	Z score = 0.506 *P* value = 0.613		Insignificant	Z score = −0.662 *P* value = 0.508		Insignificant
−90 kPa before versus −90 kPa after	Z score = 1.994 *P* value = 0.0462		Significant	Z score = 1.752 *P* value = 0.0798		Insignificant	Z score = 1.591 *P* value = 0.112		Insignificant

*%Difference = ((After − Before) / Before) × 100

decrease in tan δ at low temperatures. This effect could be beneficial for applications requiring greater creep-resistant wood. Recent research has shown a direct relationship between the suppression of viscous properties and the increase in creep resistance (Gray et al. 2009). In contrast, the ATM and − 30 kPa samples showed a significant increase in tan δ, which can be useful for applications where vibration or sound damping properties are needed (Brémaud et al. 2010).

Conclusion

This research has demonstrated that SiO_2 impregnation can simultaneously reduce water uptake capacity and improve the mechanical properties of spruce wood if it is performed under vacuum pressure. However, the impregnation needs to be conducted at elevated vacuum pressure so that the change of the properties will become statistically significant. Various characterization methods such as pycnometry, tensiometry, SEM, TEM, TGA, DMA, and statistical analyses were used to determine the optimal vacuum pressure condition.

The results showed that all impregnation conditions were able to significantly decrease the water uptake capacity of the wood in comparison with the non-treated samples. However, the impregnated samples did not exhibit a significant change in R_m, except for the SiO_2 samples impregnated under a vacuum pressure of − 90 kPa.

The density of the samples impregnated under vacuum was higher than those treated under atmospheric conditions, which was congruous with the water uptake results that indicated the reduction in void of the wood samples that led to a considerable decrease in water uptake capacity. However, the results revealed that the effectiveness of the impregnation is significant when performed at − 90 kPa pressures. This outcome was confirmed by performing electron microscopy on the samples. The micrographs showed that a vacuum pressure of − 90 kPa was required to homogeneously disperse SiO_2 nanoparticles in the vascular system of the wood.

DMA tests along with TGA and microscopic analyses revealed that SiO_2 impregnation under vacuum pressure is subject to two competing mechanisms. On the one hand, the vacuum helps the SiO_2 particles (the solid phase of the colloid) diffuse and disperse into the vascular system of the wood. On the other hand, this process exposes the inner structure of the wood to an alkaline solution. Accordingly, vacuum impregnation can cause a degradation-solubilization phenomenon due to the alkaline nature of the colloid. However, the extent of this side effect is dependent on the strength of the vacuum, and thus on the dispersion of SiO_2 particles in the structure of the wood. The side effect can be partially or completely compensated by the addition of SiO_2 nanoparticles depending on the strength of the vacuum to uniformly disperse the particles into the wood structure, as shown in the − 90 kPa samples. A detailed investigation of the viscoelastic properties showed that a vacuum pressure of − 90 kPa could induce the full recovery and improve the storage and loss modulus of wood. The − 90 kPa samples were effectively impregnated and had a uniform dispersion of SiO_2 particles in the lumens, which reinforced wood and caused the dissipation of energy through particle–particle and particle-lumen wall frictions when the samples

underwent deformations. On the other hand, at vacuum pressures of − 60 kPa and − 30 kPa, the impregnation was unable to have a statistically significant effect on the viscoelastic properties. Moreover, the impregnation under atmospheric conditions did not allow the colloid to permeate inside the wood structure and thus resulted in the formation of a solid film. The film reinforced the sample and increased the dissipation of energy through stick–slip oscillation. SiO_2 impregnation under atmospheric conditions could be useful in the development of materials that require vibration reduction or sound damping properties, whereas vacuum impregnation under − 90 kPa could be advantageous for improving the creep resistance of spruce wood.

Supplementary Information The online version contains supplementary material available at https://doi.org/10.1007/s00226-022-01448-0.

Acknowledgements Not applicable.

Authors' Contributions ML-P: Writing – Original draft preparation, conducting a research and investigation process, analyze and synthesize study data. CAB: Writing – Original draft preparation, conducting a research and investigation process. RF: Conceptualization, methodology, resources, writing – review and editing, supervision, funding acquisition. MR: Writing – Original draft preparation.

Funding The authors gratefully acknowledge the financial support received from the Natural Sciences and Engineering Research Council of Canada (NSERC).

Declarations

Conflict of interest The authors declare that they have no known competing financial interests or personal relationships that could have appeared to influence the work reported in this paper.

Availability of data and materials Not applicable.

References

Bak M, Molnár F, Németh R (2018) Improvement of dimensional stability of wood by silica nanoparticles. Wood Mater Sci Eng 14(11):1–11. https://doi.org/10.1080/17480272.2018.1528568

Beaulieu D, Biermeier D (2020) How to Seal a Deck With Thompson's WaterSeal. The Spruce. https://www.thespruce.com/seal-a-deck-with-thompsons-water-seal-2131998. Accessed 26 June 2021

Borůvka V, Ziedler A, Doubek S (2016) Impact of silicon-based chemicals on selected physical and mechanical properties of wood. Wood Res 61(4):513–524

Boulos L, Foruzanmehr MR, Tagnit-Hamou A et al (2017) Wetting analysis and surface characterization of flax fibers modified with zirconia by sol-gel method. Surf Coat Tech 313:407–416. https://doi.org/10.1016/j.surfcoat.2017.02.008

Brémaud I, Minato K, Langbour P et al (2010) Physico-chemical indicators of inter-specific variability in vibration damping of wood. Ann for Sci. https://doi.org/10.1051/forest/2010032

Brunner M (2000) On the plastic design of timber beams with a complex cross-section. Paper presented at the World Conference on Timber Engineering, British Columbia, Canada, July 31–August 3 2000

Burrows J (2013) Canadian wood-frame house construction, 3rd edn. Canada Mortgage and Housing Corporation, Ottawa, Canada

Callister WD Jr, Rethwisch DG (2018) Materials science and engineering: an introduction, 10th edn. Wiley, Hoboken, NJ

da Silva MR, Fumes BH, Nazario CED, Fernando ML (2017) Chapter eighteen - new materials for green sample preparation: recent advances and future trends. Compr Anal Chem 76:575–599. https://doi.org/10.1016/bs.coac.2017.03.003

Denes AR, Tshabalala MA, Rowell R et al (1999) Hexamethyldisiloxane-plasma coating of wood surfaces for creating water repellent characteristics. Holzforschung 53(3):318–326. https://doi.org/10.1515/hf.1999.052

Di Blasi C, Galgano A, Branca C (2009) Influences of the chemical state of alkaline compounds and the nature of alkali metal on wood pyrolysis. Ind Eng Chem Res 48:3359–3369. https://doi.org/10.1021/ie801468y

Ferry JD (1980) Viscoelastic properties of polymers, 3rd edn. Wiley, New York

Foruzanmehr MR, Boulos L, Vuillaume PY et al (2017) The effect of cellulose oxidation on interfacial bonding of nano-TiO2 coating to flax fibers. Cellulose 24:1529–1542. https://doi.org/10.1007/s10570-016-1185-6

Gray A, Orecchia D, Beake BD (2009) Nanoindentation of advanced polymers under non-ambient conditions: creep modelling and tan delta. J Nanosci Nanotechnol 9(7):4514–4519. https://doi.org/10.1166/jnn.2009.M86

Greer L, Pemberton S (2020) Water's effect on the mechanical behaviour of wood. Dissemination of IT for the Promotion of Materials Science (DoITPoMS). University of Cambridge. https://www.doitpoms.ac.uk/tlplib/wood/water_effect.php. Accessed 26 June 2021

Grosse C, Noël M, Thévenom MF, Rautkari L, Gérardin P (2018) Influence of water and humidity on wood modification with lactic acid. J Renew Mater 6(3):259–269. https://doi.org/10.7569/JRM.2017.634176

Illston JM, Domone P (2001) Construction materials – their nature and behavior, 3rd edn. CRC Press, London

Irle M, Sernek M, Thoemen H (2010) Wood-based panels – an introduction for specialists. Brunel University Press, London

Jiang J, Cao J, Wang W (2018) Characteristics of wood-silica composites influenced by the pH value of silica sols. Holzforschung 72(4):311–319. https://doi.org/10.1515/hf-2017-0126

Lin LY, Feng F (2012) The composite wood impregnated with silicon sol solution. Adv Mat Res 466–467:121–126. https://doi.org/10.4028/www.scientific.net/amr.466-467.121

Livingston EH (2004) Who was student and why do we care so much about his T-test? J Surg Res 118:58–65. https://doi.org/10.1016/j.jss.2004.02.003

Luft JH (1961) Improvements in epoxy resin embedding methods. J Biophys Biochem Cytol 9:409–414. https://doi.org/10.1083/jcb.9.2.409

Martins JAC, Oden JT, Simões FMF (1990) A study of static and kinetic friction. Int J Eng Sci 28(1):29–92. https://doi.org/10.1016/0020-7225(90)90014-A

Olsson A-M, Salmén L (1997) The effect of lignin composition on the viscoelastic properties of wood. Nord Pulp Pap Res J 12:140–144. https://doi.org/10.3183/npprj-1997-12-03-p140-144

Prošek Z, Králík V, Topič J et al (2015) A description of the microstructure and the micromechanical properties of spruce wood. Acta Polytech 55:39–49. https://doi.org/10.14311/ap.2015.55.0039

Przystupa K, Pieniak D, Samociuk W et al (2020) Mechanical properties and strength reliability of impregnated wood after high temperature conditions. Materials 13(23):5521. https://doi.org/10.3390/ma13235521

Rowell RM, Banks WB (1985) Water repellency and dimensional stability of wood. For Prod Lab. https://doi.org/10.2737/fpl-gtr-50

Shi X, Dalai NS, Hu XN, Vallyathan V (1989) The chemical properties of silica particle surface in relation to silica-cell interactions. J Toxicol Environ Health 27:435–454. https://doi.org/10.1080/15287398909531314

UPLAND (2017) Wood for Mid-rise Construction. Atlantic Wood*WORKS!*. https://wood-works.ca/wp-content/uploads/160601-Wood-4-Mid-Rise-Report-FINAL-2017-03-28-sm.pdf. Accessed 26 June 2021

Williams RS, Feist WC (1999) Water repellents and water-repellent preservatives for Wood. For Prod Lab. https://doi.org/10.2737/fpl-gtr-109

Xu E, Zhang Y, Lin L (2020) Improvement of mechanical, hydrophobicity and thermal properties of Chinese fir wood by impregnation of nano silica sol. Polymers 12(8):1632. https://doi.org/10.3390/polym12081632

Zhang N, Xu M, Cai L (2019) Improvement of mechanical, humidity resistance and thermal properties of heat-treated rubber wood by impregnation of SiO_2 precursor. Sci Rep 9:982. https://doi.org/10.1038/s41598-018-37363-3